ANESTHESIOLOGY

Brainstem Modulation of Nociception by Periaqueductal Gray Neurons Expressing the μ-Opioid Receptor in Mice

Eileen Nguyen, M.D., Ph.D., Michael C. Chiang, M.D., Ph.D., Catherine Nguyen, B.S., Sarah E. Ross, Ph.D.

Anesthesiology 2023; 139:462–75

EDITOR'S PERSPECTIVE

What We Already Know about This Topic

- The periaqueductal gray in the mesencephalon is a major component of the endogenous opioid system and is involved in the coordination of autonomic and behavioral responses to noxious input
- The question of how different neuronal populations, expressing μ-opioid receptors, in the periaqueductal gray modulate nociceptive responses is incompletely explored

What This Article Tells Us That Is New

- Selective opto- and chemogenetic activation of μ-opioid receptor–expressing neurons of the periaqueductal gray in mice facilitated escape behaviors but inhibited reflexive responses to thermal and mechanical stimuli or itch behavior
- These laboratory observations suggest that μ-opioid receptor–expressing neurons of the periaqueductal gray modulate nociception by eliciting distinct escape and reflexive responses

ABSTRACT

Background: Pharmacologic manipulations directed at the periaqueductal gray have demonstrated the importance of the μ-opioid receptor in modulating reflexive responses to nociception. The authors hypothesized that a supraspinal pathway centered on neurons in the periaqueductal gray containing the μ-opioid receptor could modulate nociceptive and itch behaviors.

Methods: The study used anatomical, optogenetic, and chemogenetic approaches in male and female mice to manipulate μ-opioid receptor neurons in the periaqueductal gray. Behavioral assays including von Frey, Hargreaves, cold plantar, chloroquine-induced itch, hotplate, formalin-induced injury, capsaicin-induced injury, and open field tests were used. In separate experiments, naloxone was administered in a postsurgical model of latent sensitization.

Results: Activation of μ-opioid receptor neurons in the periaqueductal gray increased jumping (least-squares mean difference of –3.30 s; 95% CI, –6.17 to –0.44; $P = 0.023$; n = 7 or 8 mice per group), reduced itch responses (least-squares mean difference of 70 scratching bouts; 95% CI, 35 to 105; $P < 0.001$; n = 8 mice), and elicited modestly antinociceptive effects (least-squares mean difference of –0.7 g on mechanical and –10.24 s on thermal testing; 95% CI, –1.3 to –0.2 and 95% CI, –13.77 to –6.70, and $P = 0.005$ and $P < 0.001$, respectively; n = 8 mice). Last, the study uncovered the role of the periaqueductal gray in suppressing hyperalgesia after a postsurgical state of latent sensitization (least-squares mean difference comparing saline and naloxone of –12 jumps; 95% CI, –17 to –7; $P < 0.001$ for controls; and –2 jumps; 95% CI, –7 to 4; $P = 0.706$ after optogenetic stimulation; n = 7 to 9 mice per group).

Conclusions: μ-Opioid receptor neurons in the periaqueductal gray modulate distinct nocifensive behaviors: their activation reduced responses to mechanical and thermal testing, and attenuated scratching behaviors, but facilitated escape responses. The findings emphasize the role of the periaqueductal gray in the behavioral expression of nociception using reflexive and noxious paradigms.

(Anesthesiology 2023; 139:462–75)

Several supraspinal structures, including the periaqueductal gray, are involved in coordinating autonomic and behavioral responses to noxious input, which can include either the inhibition or facilitation of nociceptive responses.[1,2] The periaqueductal gray, which is a major component of the endogenous opioid system, has been shown to modulate nociception through a descending pathway involving the rostral ventromedial medulla and spinal cord.[3]

This article is featured in "This Month in Anesthesiology," page A1. Supplemental Digital Content is available for this article. Direct URL citations appear in the printed text and are available in both the HTML and PDF versions of this article. Links to the digital files are provided in the HTML text of this article on the Journal's Web site (www.anesthesiology.org). E.N. and M.C.C. contributed equally to this article.

Submitted for publication April 25, 2023. Accepted for publication June 22, 2023. Published online first on June 26, 2023.

Eileen Nguyen, M.D., Ph.D.: Department of Anesthesiology, University of Pittsburgh School of Medicine, Pittsburgh, Pennsylvania; Department of Neurobiology, University of Pittsburgh, Pittsburgh, Pennsylvania; Department of Anesthesiology, University of California-Los Angeles, Los Angeles, California.

Michael C. Chiang, M.D., Ph.D.: Department of Anesthesiology, University of Pittsburgh School of Medicine, Pittsburgh, Pennsylvania; Department of Neurobiology, University of Pittsburgh, Pittsburgh, Pennsylvania.

Catherine Nguyen, B.S.: Department of Anesthesiology, University of Pittsburgh School of Medicine, Pittsburgh, Pennsylvania; Department of Neurobiology, University of Pittsburgh, Pittsburgh, Pennsylvania.

Sarah E. Ross, Ph.D.: Department of Anesthesiology, University of Pittsburgh School of Medicine, Pittsburgh, Pennsylvania; Department of Neurobiology, University of Pittsburgh, Pittsburgh, Pennsylvania.

 Anesthesiology 2023; 139:462–75. DOI: 10.1097/ALN.0000000000004668

<zdoi;10.1097/ALN.0000000000004668>

In particular, periaqueductal gray circuits have been proposed to underlie offset analgesia, conditioned pain modulation, and placebo analgesia in human subjects.[4–6] Thus, a major emphasis of translational and clinical work on nociceptive pathways has focused on the modulatory actions of periaqueductal gray pathways.

Pharmacologic manipulations of the periaqueductal gray have provided critical insight into the types of receptors that participate in the descending modulation of nociception. For example, the injection of a μ-opioid receptor agonist, such as DAMGO or morphine, into the periaqueductal gray results in the elevation of sensory thresholds.[7–9] Local microinjection of the μ antagonist, naloxone, into the periaqueductal gray or lesioning of the periaqueductal gray has blocked the antinociceptive effects of systemic morphine.[9,10] These studies identify the periaqueductal gray as a crucial site of action for the effects of local as well as systemically administered opioids.

It has been proposed that inhibitory neurons within the periaqueductal gray express the μ-opioid receptor,[11,12] suggesting that μ-opioid receptor agonists produce antinociception through the disinhibition of periaqueductal gray output.[11,13,14] In support of this model, immunohistochemistry shows that μ-opioid receptor–expressing periaqueductal gray (PAG^{MOR}) neurons make up a subset of all periaqueductal gray γ-aminobutyric acid–mediated (GABAergic) neurons that do not project to the rostral ventromedial medulla.[15–17] However, other studies have also shown that PAG^{MOR} neurons compose more than half of rostral ventromedial medulla–projecting cells.[15] Thus, it remains unclear whether the antinociceptive effects of opioid microinjections into the periaqueductal gray are mediated through the inhibition of local interneurons, rostral ventromedial medulla–projecting periaqueductal gray neurons, or both. Selective manipulation of periaqueductal gray circuits has posed challenges due to the molecular complexity of neurons in the periaqueductal gray. More recently, advancements in genetic tools using Cre drivers have enabled investigators to more accurately characterize the modulatory roles of different neuronal periaqueductal gray populations in response to distinct somatosensory modalities.[18–21]

The role of the periaqueductal gray in the descending modulation of nociception is thought to occur through its ability to coordinate appropriate motor responses to nociception in rodents.[22,23] We have previously shown that parabrachial nucleus projections to the periaqueductal gray are important for the escape component of the pain response, which includes running and jumping behaviors.[24] Furthermore, it was recently shown that in different contexts, the periaqueductal gray differentially modulates either antinociception or locomotion.[25] Here, we set out to characterize the neurons in the periaqueductal gray that express μ-opioid receptor and examine the effect of manipulating these neurons in a variety of nociceptive tests.

Materials and Methods

Mice

All animals were of the C57BL/6J background. MOR^{Cre} mice were a generous gift from Richard Palmiter, Ph.D. (University of Washington, Seattle, Washington) and are now available on Jax #034475. The studies were performed in both male and female mice 8 to 10 weeks of age (20 to 35 g mice). Male and female mice were used for all experiments, and data were pooled. For behavioral experiments, animal groups were not always evenly balanced across male and female subjects due to variations in litter sizes and distributions of sex across litters. Animals were randomly assigned to treatment groups. For neurochemical analyses, three or four mice per group were used (immunohistochemistry) and three or four sections from each mouse were averaged from three mice in total for fluorescent *in situ* hybridization. For optogenetic and chemogenetic behavioral testing, 6 to 11 mice per group were used. Mice were given free access to food and water and housed under standard laboratory conditions. The use of animals was approved by the Institutional Animal Care and Use Committee of the University of Pittsburgh (Pittsburgh, Pennsylvania; protocol No. 14043431).

Viral Vectors

All viruses used in this study are commercially available from UNC Vector Core (USA) and Addgene (USA). These were AAV2.hSyn.DIO.hM4D(Gi)-mCherry (titer: 1.5×10^{13}), AAV2-hsyn-DIO-mCherry (titer: 1.2×10^{13}), AAV2-hsyn-DIO-hM3D(Gq)-mCherry (titer: 8.6×10^{12}), AAV2/EF1a-DIO-hChR^2(H134R)-eYFP (titer: 4.0×10^{12}), AAV2.EF1a.DIO.eYFP (titer: 9.5×10^{12}), and AAVr-hsyn-DIO-mCherry (titer: 7.0×10^{12}).

Stereotaxic Injections and Optical Fiber Implantation

Animals were anesthetized with 2% isoflurane and placed in a stereotaxic head frame. A custom-made metal needle (33-gauge) loaded with virus was delivered to the injection site. Virus was infused at a rate of 100 nl/min using a Hamilton syringe with a micro-syringe pump (World Precision Instruments, USA). Mice received 250 to 500 nl virus. The injection needle was left in place for an additional 5 min and then slowly withdrawn during another 5 min. Injections and cannula implantations were performed at the following coordinates: rostral ventromedial medulla, anterior-posterior −5.80 mm, medial-lateral 0.00 mm, and dorsal-ventral −6.00; and periaqueductal gray, anterior-posterior −4.70 mm, medial-lateral ± 0.74 mm, and dorsal-ventral −2.75 (bilaterally). For implantation of optical fibers (Thor Labs: 1.25 mm ceramic ferrule, 230 mm diameter), implants were slowly lowered 0.3 to 0.5 mm above the site of injection and secured to the skull with a thin layer of Vetbond (3M, USA) and dental cement. The incision was

closed using Vetbond, and animals were provided analgesics (ketoprofen, intraperitoneal, 10 mg/kg; buprenorphine, subcutaneous, 0.3 mg/kg) and allowed to recover over a heating pad. Mice were given 4 weeks to recover before experimentation.

Pharmacologic Agents

Clozapine N-oxide (Tocris, Bristol, United Kingdom) was dissolved in phosphate buffer solution and administered intraperitoneally (5 mg/kg). Animals received clozapine N-oxide across multiple days to complete behavioral testing, with at least 1 day in between assays. Capsaicin (0.1%) in 10% ethanol in phosphate buffer solution was injected 10 μl into the plantar hind paw (n = 6 to 8 mice per group). Formalin (Sigma, USA; 2% w/v) in saline was injected 10 μl into the plantar hind paw (n = 11 to 13 mice per group). Chloroquine diphosphate salt (Sigma) was dissolved in physiologic saline (100 μg in 10 μl) and administered intradermally (n = 6 to 9 mice per group).

Fluorescent *In Situ* Hybridization

Mice were anesthetized with an intraperitoneal injection of urethane and euthanized by decapitation. Multiplex fluorescent *in situ* hybridization was performed according to the manufacturer's instructions (Advanced Cell Diagnostics, USA; No. 320850). Briefly, 14-μm-thick fresh frozen sections containing the rostral ventromedial medulla were fixed in 4% paraformaldehyde, dehydrated, treated with protease for 15 min, and hybridized with gene-specific probes to mouse. Probes were used to detect Probe-tdTomato-C2 (No. 317041-C2), mCherry-C2 (No. 431201), Mm-Oprm1-C1 (No. 315841), Mm-Slc32a1-C3 (No. 319191; glutamatergic neurons), and Mm-Slc17a6-C3 (No. 319171; GABAergic neurons). 4′,6-diamidino-2-phenylindole (DAPI; No. 320858) was used to visualize nuclei. 3-Plex positive (No. 320881) and negative (No. 320871) control probes were tested. One animal was excluded from the analysis due to poor tissue quality in the periaqueductal gray for the glutamatergic or GABAergic characterization study as well as the retrograde characterization study. Three to four z-stacked sections were quantified for a given mouse, and three mice were used per experiment.

Immunohistochemistry

Mice were anesthetized with an intraperitoneal injection of urethane, transcardially perfused, and postfixed for at least 4 h in 4% paraformaldehyde. Brain sections 40 μm thick were collected on a cryostat for immunohistochemistry. Sections were blocked at room temperature for 2 h in 5% donkey serum, 0.2% Triton, in phosphate buffered saline. Primary antisera were incubated for 14 h overnight at 4°C: rabbit anti-red fluorescent protein (1:1,000), chicken anti-green fluorescent protein (1:1,000), and mouse anti-NeuN (1:500). Sections were subsequently washed three times for 20 min in wash buffer (0.2% Triton, in phosphate buffer solution) and incubated in secondary antibodies (Life Technologies, 1:500; USA) at room temperature for 2 h. Sections were then incubated in Hoechst (Thermo Fisher, 1:10,000; USA) for 1 min and washed three times for 15 min in wash buffer, mounted, and coverslipped.

Fos Experiments

Mice received either optical stimulation or clozapine N-oxide for Fos analysis. Brain tissues were harvested 90 min after for immunohistochemistry. For optogenetically induced Fos expression, mice were photostimulated for 20 min at a 3 s on, 2 s off stimulation pattern. Mice received clozapine N-oxide as described for behavioral experimentation. Animals were perfused 90 min after the initial onset of photostimulation or after clozapine N-oxide administration for immunohistochemistry.

Image Acquisition and Quantification

Full-tissue thickness sections were imaged using either an Olympus BX53 fluorescent microscope with UPlanSApo 4×, 10×, or 20× objectives or a Nikon A1R confocal microscope with 20× or 60× objectives. All images were quantified and analyzed using ImageJ. To quantify images in fluorescent *in situ* hybridization experiments, confocal images of tissue samples (three or four sections averaged per mouse over three or four mice) were imaged, and only cells whose nuclei were clearly visible by DAPI staining and exhibited a fluorescent signal were counted. To quantify Fos-labeled cells, sections of the entire rostral ventromedial medulla or periaqueductal gray were imaged using fluorescent microscopy, and images were manually counted.

Behavior

All assays were performed in the Pittsburgh Phenotyping Core (Pittsburgh, Pennsylvania) and scored by an experimenter blind to treatment. For all chemogenetic behavioral experiments, clozapine N-oxide was administered (5 mg/kg intraperitoneal) 30 min before the start of behavioral testing. Animals in chemogenetic studies were subjected to testing in the following order of assays: open field, von Frey, Hargreaves, chloroquine-induced scratching, tail flick, capsaicin, and formalin. Mice tested using optogenetics were photostimulated with the following parameters: 10 mW laser power, 20 Hz stimulation frequency, and 5 ms pulse duration. Repeat testing with either chemogenetics or optogenetics was completed at 1 day intervals to minimize exposure to clozapine N-oxide and optical stimulation, respectively.

Observation of Scratching Behavior

Mice were individually placed in the observation cage (12 × 9 × 14 cm) to permit acclimation for 30 min. Scratching behavior was videotaped for 30 min after the

administration of chloroquine into the nape of the neck. The total number of scratch bouts by the hind paws directed to the neck during this period was counted.

Hargreaves Testing

Animals were acclimated on a glass plate held at 30°C (Model 390 Series 8, IITC Life Science Inc.). A radiant heat source was applied to the hind paw, and latency to paw withdrawal was recorded. Two trials were conducted on each paw, with at least 5 min between testing the opposite paw and at least 10 min between testing the same paw. To avoid tissue damage, a cutoff latency of 20 s was set. Values from both paws were averaged to determine withdrawal latency.

von Frey Testing

Mechanical sensitivity was measured using the Chaplan up-down method of the von Frey test. Calibrated von Frey filaments (North Coast Medical Inc., USA) were applied to the plantar surface of the hind paw. Lifting, shaking, and licking were scored as positive responses to von Frey stimulation. Average responses were obtained from each hind paw, with 3 min between trials on opposite paws, and 5 min between trials on the same paw.

Tail-flick Assay

Mice were placed in custom-made mouse restraints and allowed to habituate for 15 min before testing. Tails were immersed 3 cm into a water bath at 48° and 55°C, and the latency to tail-flick was measured three times with a 1 min interval between trials. For optogenetic testing, mice were photostimulated for 10 s before testing. Cutoff times were implemented at 25 s (48°) and 5 s (55°C) to prevent tissue damage.

Hotplate

Mice were placed on a 55°C hotplate, and the latency to the first escape response (jump) and the total number of jumps were measured during a 60 s period. Values were averaged across two trials for each mouse spaced several minutes apart. For optogenetic testing, mice were photostimulated for 10 s before testing. For experiments assessing latent sensitization, naloxone (10 mg/kg intraperitoneal) was administered 30 min before photostimulation.

Open Field

Spontaneous activity in the open field was conducted during 30 min in an automated Versamax Legacy open-field apparatus for mice (Omnitech Electronics Incorporated, USA). Distance traveled was measured by infrared photo beams located around the perimeter of the arenas interfaced to a computer running Fusion v.6 for Versamax software (Omnitech Electronics Incorporated), which monitored the location and activity of the mouse during testing. Activity plots were generated using the Fusion Locomotor Activity Plotter analyses module (Omnitech Electronics Incorporated). Mice were placed into the open field 30 min after clozapine N-oxide injection.

Acute Injury Models

For formalin-induced injury, 10 μl 2% formalin was injected into the intraplantar hind paw. Mice were video recorded for 1 h after formalin injection, and time spent licking and lifting the paw was scored in 5-min bins. For capsaicin-induced injury, animals received 10 μl intraplantar capsaicin (0.1% w/v in 10% ethanol diluted in saline), and the total time spent licking the injured paw was quantified during 20 min. Hargreaves and von Frey testing after capsaicin-induced injury occurred 20 min and 1 h after intraplantar injection.

Statistical Analysis

Statistical analyses were performed using GraphPad Prism 9. Values are presented as mean ± SD. N refers to the number of mice. In neurochemical experiments, multiple technical replicates were averaged for individual mice. Statistical significance was assessed using tests indicated in applicable figure legends including the two-tailed, unpaired *t* test (to compare Fos expression and nocifensive behaviors in mice treated with control vector compared to channel rhodopsin-injected mice), one-way ANOVA with Dunnett's multiple comparisons test (in chemogenetic studies to compare animals receiving the control vector, the inhibitory chemogenetic actuator, or the excitatory chemogenetic actuator), or two-way repeated-measures ANOVA with Sidak's multiple comparisons test (in chemogenetic and optogenetic studies where control or experimental groups were compared before and after treatment such as with naloxone or clozapine N-oxide). Significance was indicated by $P < 0.05$. Sample sizes were based on pilot data and are similar to those typically used in the field. No formal *a priori* statistical power calculation was conducted. Data were determined to be normally distributed by the Shapiro-Wilks test.

Results

Molecular and Anatomical Characterization of Neurons in the Periaqueductal Gray Containing the μ-Opioid Receptor

To visualize the μ-opioid receptor–expressing neurons in the periaqueductal gray, we injected an adeno-associated virus encoding a Cre-dependent fluorescent reporter into the periaqueductal gray of MOR^{Cre} mice (fig. 1A). We found that PAG^{MOR} neurons project to numerous structures in the forebrain and brainstem such as the anterior hypothalamus, ventral tegmental area, and rostral ventromedial medulla (fig. 1, A and B).

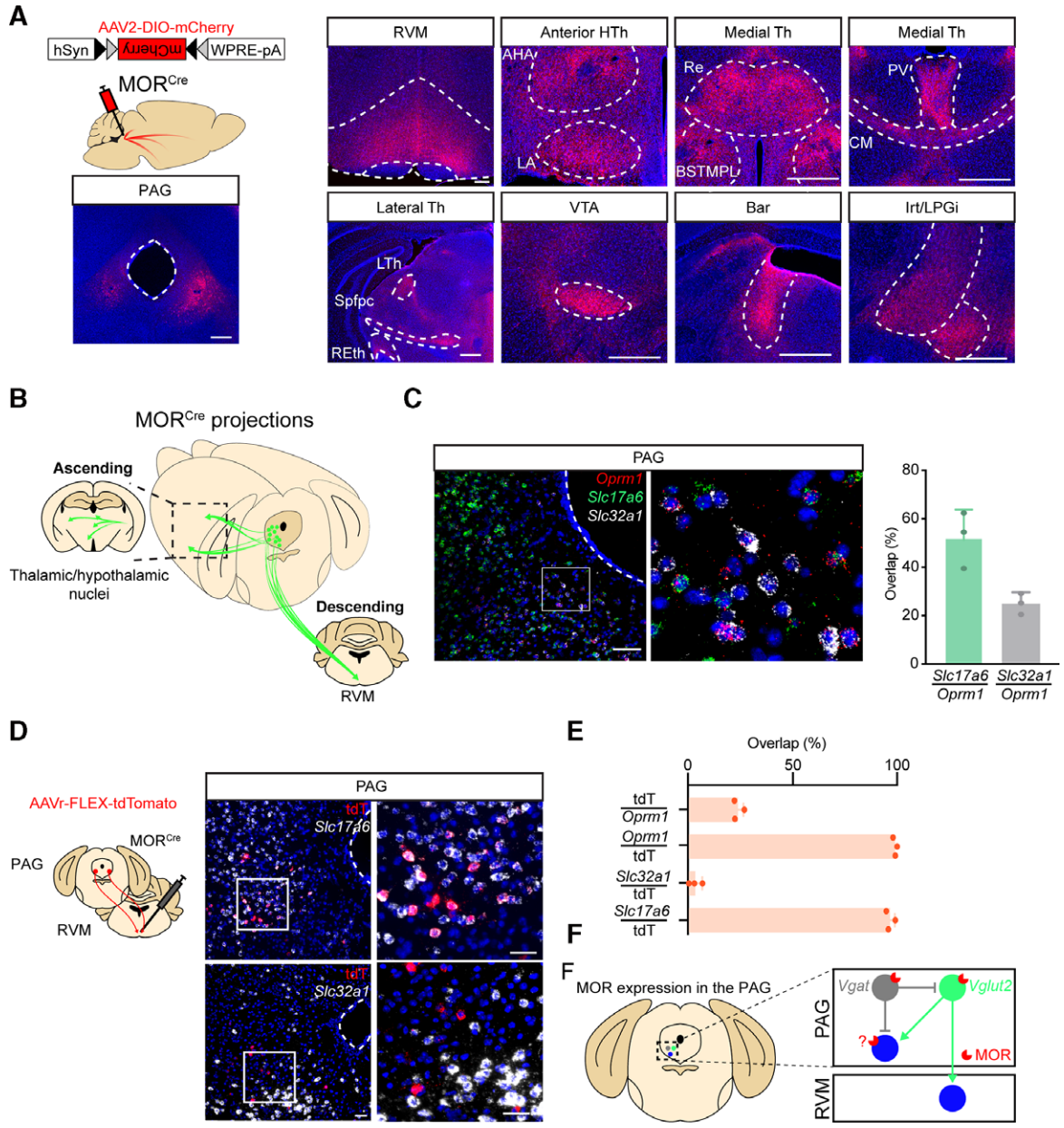

Fig. 1. Molecular and anatomic characterization of μ-opioid receptor neurons in the periaqueductal gray. (*A*) Approach to visualize projections from μ-opioid receptor (MOR) neurons in the periaqueductal gray (PAG^{MOR}) using Cre-dependent tracers introduced into the periaqueductal gray (PAG). Major downstream targets of PAG^{MOR} neurons throughout the brain and brainstem. Representative images are shown. *Scale bar* = 100 μm. (*B*) Cartoon representation of PAG^{MOR} ascending and descending projections throughout the brain. (*C*) Fluorescent *in situ* hybridization (FISH) characterization of *Oprm1* (μ-opioid receptor) in PAG neurons with respect to excitatory (*Slc17a6* or Vglut2) and inhibitory (*Slc32a1* or Vgat) markers. *Scale bar* = 100 μm. Quantification is shown on the *right*. Data are mean ± SD with *dots* representing individual mice (n = 3 mice, with an average of 3 or 4 sections per mouse). (*D*) Cartoon depiction of two complementary approaches used to characterize descending projections of PAG^{MOR} neurons to the rostral ventromedial medulla (RVM). Retrograde tracers are introduced into the RVM of MOR^{Cre} or wild-type mice, and labeled cell bodies in the PAG are characterized (using *Oprm1, Slc17a6*, and *Slc32a1*) using fluorescent *in situ* hybridization. Representative images of PAG sections are shown. *Scale bar* = 50 μm. (*E*) Quantification of *D*. Data are mean ± SD with *dots* representing individual mice (n = 3 mice, with an average of 3 or 4 sections per mouse). (*F*) Model for the expression of MOR in PAG neurons. Excitatory and inhibitory PAG neurons containing MOR may coordinate nociceptive and defensive behaviors. AHA, anterior hypothalamic area; Bar, Barrington's nucleus; BSTMPL, bed nucleus stria terminalis, medial posterolateral; CM, centromedial thalamic nucleus; Irt, intermediate reticular nucleus; LA, lateroanterior nuclei; LPGi, lateral paragigantocellular nucleus; PR, prerubral thalamic area; PV, paraventricular thalamic nucleus; Re, reuniens thalamic nucleus; REth, retroethmoid intramedullar thalamic area; RRF, retrorubral field; Spfpc, subparafascicular thalamus; VTA, ventral tegmental area.

Next, we used fluorescent *in situ* hybridization to characterize μ-opioid receptor neurons in the periaqueductal gray (encoded by the *Oprm1* gene). We found that *Oprm1* overlapped with both *Slc17a6*/Vglut2 (mean ± SD, 52.1 ± 11.7%) and *Slc32a1*/Vgat (25.0 ± 4.3%; fig. 1C). These observations support the idea that PAG^{MOR} neurons are heterogeneous, comprising both excitatory and inhibitory neurons as well as local and projection neurons to numerous targets. Given the important role of the periaqueductal gray in the descending modulation of nociception[9,10] and its projections to the rostral ventromedial medulla[26–28] (fig. 1A), we focused on this particular pathway. To specifically characterize PAG^{MOR} neurons projecting to the rostral ventromedial medulla, we coinjected Cre-dependent and Cre-independent retrograde tracers in the rostral ventromedial medulla of *MOR^{Cre}* and wild-type mice, respectively (fig. 1D). We then used fluorescent *in situ* hybridization to characterize back-labeled neurons in the periaqueductal gray. We found that PAG^{MOR} neurons that project to the rostral ventromedial medulla make up approximately 25% of all PAG^{MOR} neurons. In contrast to the molecular heterogeneity of *Oprm1* neurons within the periaqueductal gray, which expressed either *Slc32a1* or *Slc17a6*, PAG^{MOR} neurons that project to the rostral ventromedial medulla were found to be exclusively glutamatergic by their expression of *Slc17a6* (96.6 ± 2.3%) and limited expression of *Slc32a1* (3.1 ± 3.3%; fig. 1E). These data are consistent with the idea that local PAG^{MOR} neurons are GABAergic, whereas those that project to the rostral ventromedial medulla are glutamatergic (fig. 1F).

We then assessed the functional role of PAG^{MOR} neurons that project to the rostral ventromedial medulla using an optogenetic approach in which an adeno-associated virus encoding channelrhodopsin (or enhanced yellow fluorescent protein [eYFP]) was injected into the periaqueductal gray and optogenetic stimulation was performed in the rostral ventromedial medulla (fig. 2A). Optogenetic activation of PAG^{MOR} terminals in the rostral ventromedial medulla resulted in the robust induction of Fos expression in the rostral ventromedial medulla (mean ± SD, eYFP 25.4 ± 2.2%, compared with channelrhodopsin 56.3 ± 12.5%; mean difference, 30.89 ± 7.35; 95% CI, 10.49 to 51.29; $P = 0.014$ by unpaired *t* test; n = 3 mice per group) (fig. 2B). Behaviorally, photostimulation of PAG^{MOR} fibers within the rostral ventromedial medulla did not affect jumping responses on the hotplate (jumping mean difference, 4 ± 3 jumps; 95% CI, –2 to 11; latency to jump mean difference, –5.14 ± 4.58 s; 95% CI, –15.04 to 4.75; with $P = 0.183$ and $P = 0.282$, respectively by unpaired *t* test; n = 6 to 9 mice per group; fig. 2C, Supplemental Figure 1A, https://links.lww.com/ALN/D199). Although stimulation of PAG^{MOR} fibers in the rostral ventromedial medulla reliably induced activity in the rostral ventromedial medulla based on Fos expression, this stimulation was not sufficient to alter escape behaviors with hotplate testing.

Neurons in the Periaqueductal Gray Containing the μ-Opioid Receptor Modulate Complex Somatosensory Behaviors

We tested the contributions of PAG^{MOR} neurons directly by using a chemogenetic approach to target them. We activated and inhibited PAG^{MOR} neurons by injection of AAV2.hSyn.DIO.hM3Dq-mCherry and AAV2.hSyn.DIO.hM4Di-mCherry, respectively, into the periaqueductal

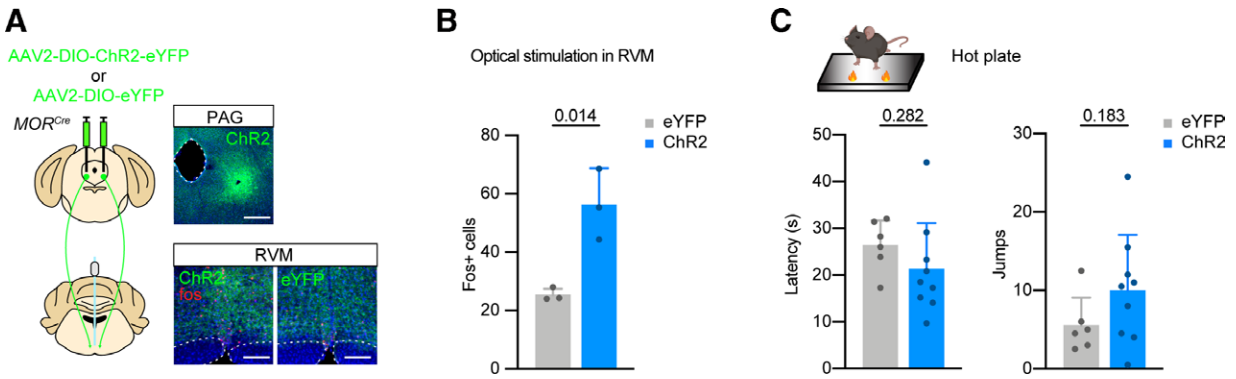

Fig. 2. Optogenetic manipulation of μ-opioid receptor (MOR)–containing projections from the periaqueductal gray (PAG) within the rostral ventromedial medulla (RVM). (*A*) Approach to optogenetically activate MOR–containing projections from the PAG (PAG^{MOR}) in the rostral ventromedial medulla. The activation of PAG^{MOR} terminals within the RVM induces the expression of Fos in the RVM. *Scale bars* = 200 μm. (*B*) Quantification of *A*. Data are mean ± SD with *dots* representing individual mice (n = 3 mice, with an average of 3 or 4 sections per mouse). *P* value represents the result of a two-tailed, unpaired *t* test. Representative images from control and channelrhodopsin (ChR2) mice. (*C*) The effect of optogenetic activation of PAG projections in the RVM on jumping behaviors on the hotplate assay (total jumps and latency to jump). Data are mean ± SD with *dots* representing individual mice (n = 6 to 9 mice per group). *P* values represent the result of a two-tailed, unpaired *t* test.

gray of MOR^{Cre} mice. As a validation of these chemogenetic actuators, we confirmed that chemogenetic activation of PAG^{MOR} neurons resulted in the induction of Fos expression in the periaqueductal gray (control compared to chemogenetic activation mean difference of –355 cells; 95% CI, –433 to –277; $P < 0.001$ by 1-way ANOVA with Dunnett's multiple comparisons test; n = 7 or 8 mice per group) (fig. 3A). In addition, we found that the chemogenetic activation of PAG^{MOR} neurons increased the number of Fos-expressing cells in the rostral ventromedial medulla (control compared to chemogenetic activation mean difference of –31 cells; 95% CI, –39 to –23; $P < 0.001$ by one-way ANOVA with Dunnett's multiple comparisons test; n = 7 or 8 mice per group; fig. 3B), as seen previously upon optogenetic stimulation of PAG^{MOR} terminals in the rostral ventromedial medulla. Neither activation nor inhibition of PAG^{MOR} neurons affected locomotor activity in an open field assay (fig. 3C; Supplemental Figure 2A, https://links.lww.com/ALN/D200), suggesting that the manipulation of PAG^{MOR} neurons does not influence locomotion (control compared with chemogenetic activation: mean difference, –178.0 cm; 95% CI, –2,604 to 2,248; control compared with chemogenetic inhibition: mean difference, –835.7 cm; 95% CI, –3,341 to 1,670; $P = 0.978$ and $P = 0.645$, respectively, by one-way ANOVA with Dunnett's multiple comparisons test; n = 7 or 8 mice per group). To examine the role of PAG^{MOR} neurons in nociceptive behaviors, we tested mice in several assays, including hotplate (55°C) and injury models using intraplantar formalin (2% w/v in saline in 10 μl) and capsaicin (using 0.1% w/v capsaicin dissolved in 10% ethanol and saline in 10 μl). When naive mice were tested in the hotplate assay, the chemogenetic activation of PAG^{MOR} neurons increased the number of jumps relative to controls (least-squares mean difference of –3 jumps; 95% CI, –6 to –0.4; hotplate jumps in control mice compared with chemogenetic activation, $P = 0.023$ by one-way ANOVA with Dunnett's multiple comparisons test; n = 7 or 8 mice per group (fig. 3D; Supplemental Figure 2B, https://links.lww.com/ALN/D200). However, neither chemogenetic activation nor inhibition influenced licking behaviors in an acute capsaicin-induced injury model (control compared with chemogenetic activation: mean difference, –20.06 s; 95% CI, –116.2 to 76.08; control compared with chemogenetic inhibition: mean difference, 54.13 s; 95% CI, –44.38 to 152.6; $P = 0.832$ and $P = 0.333$, respectively, by one-way ANOVA with Dunnett's multiple comparisons test; n = 7 to 9 mice per group; fig. 3E, Supplemental Figure 2C, https://links.lww.com/ALN/D200). To assess the contribution of PAG^{MOR} neurons to a more persistent form of injury, we injected mice with intraplantar formalin and quantified their licking behaviors targeted to the injured paw (fig. 3F ; Supplemental Figure 2D, https://links.lww.com/ALN/D200). We found that activation of PAG^{MOR} neurons modestly increased cumulative licking responses during the second phase of the formalin assay, although this trend was not found to be statistically significant (mean difference, –83.38 s; 95% CI, –171.0 to 4.24; $P = 0.064$ by one-way ANOVA with Dunnett's multiple comparisons test; n = 11 to 13 mice per group; fig. 3G; Supplemental Figure 2E, https://links.lww.com/ALN/D200). In contrast, the inhibition of PAG^{MOR} neurons trended toward a reduction in formalin-induced licking, yet this was also not found to be statistically significant (mean difference, 73.82 s; 95% CI, –17.38 to 165.0; $P = 0.124$ by one-way ANOVA with Dunnett's multiple comparisons test; n = 11 to 13 mice per group). Together, our chemogenetic manipulations of PAG^{MOR} neurons revealed that their activation increased jumping behaviors on a noxious hotplate and licking behaviors in a model of persistent injury but did not significantly affect licking responses in response to capsaicin.

Upon testing of reflexive behaviors (fig. 4A), we found that the chemogenetic manipulations of PAG^{MOR} neurons revealed striking divergence from the behaviors we previously observed on the hotplate assay and with formalin and capsaicin-induced licking. For example, in a model of chloroquine-induced itch, chemogenetic activation of PAG^{MOR} neurons robustly attenuated scratching responses compared to baseline (least-squares mean difference of 70 scratching bouts; 95% CI, 35 to 105; $P < 0.001$ by two-way repeated-measures ANOVA with Sidak's multiple comparisons test; n = 8 mice; fig. 4B; Supplemental Figure 3A, https://links.lww.com/ALN/D201). In the von Frey assay, chemogenetic activation and inhibition of PAG^{MOR} neurons bidirectionally modulated mechanical thresholds (chemogenetic activation: least-squares mean difference, –0.7 g; 95% CI, –1.2 to –0.2; $P = 0.005$; n = 8 mice; and chemogenetic inhibition: least-squares mean difference, 0.5 g; 95% CI, –0.01 to 1.1; $P = 0.055$; n = 7 mice by two-way repeated-measures ANOVA with Sidak's multiple comparisons test; fig. 4C; Supplemental Figure 3B, https://links.lww.com/ALN/D201). In the Hargreaves assay, activation of PAG^{MOR} neurons inhibited responses to thermal thresholds (least-squares mean difference, –10.24 s; 95% CI, –13.77 to –6.70; $P < 0.001$ by two-way repeated-measures ANOVA with Sidak's multiple comparisons test; n = 8 mice; fig. 4D; Supplemental Figure 3C, https://links.lww.com/ALN/D201). However, tail flick responses were not affected by chemogenetic activation or inhibition of PAG^{MOR} neurons (chemogenetic activation: least-squares mean difference, –0.01 s; 95% CI, –1.35 to 1.33; $P > 0.999$; n = 8 mice; and chemogenetic inhibition: least-squares mean difference, –0.26 s; 95% CI, –1.53 to 0.99; $P = 0.932$; n = 9 mice by two-way repeated-measures ANOVA with Sidak's multiple comparisons test; fig. 4E; Supplemental Figure 3D, https://links.lww.com/ALN/D201).

In assays that involved frankly noxious stimulation (prolonged exposure to heat or aversive chemicals), activation of PAG^{MOR} neurons modestly facilitated jumping, which is an escape response. However, for assays that measure sensory thresholds, the von Frey and Hargreaves tests, chemogenetic

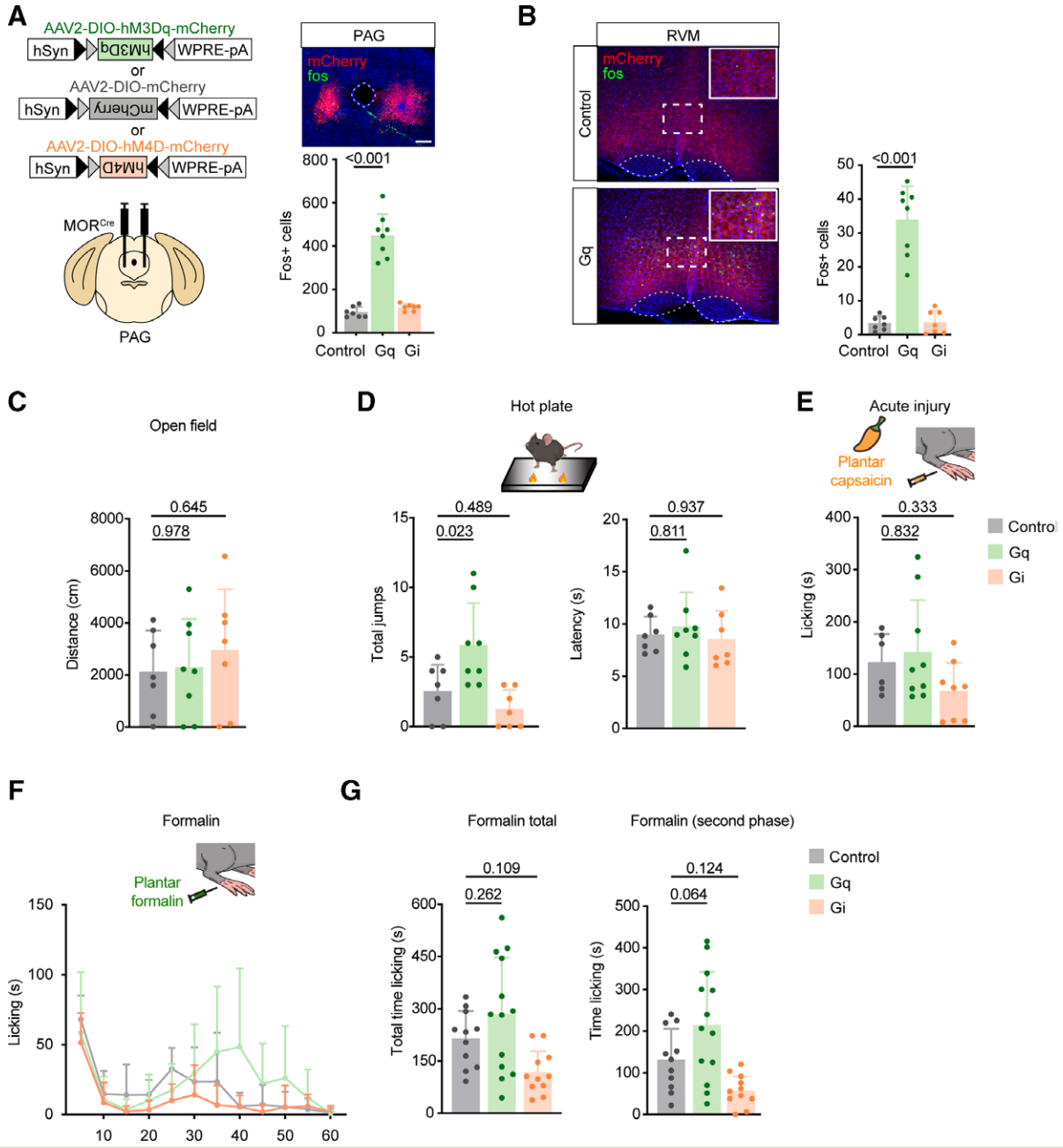

Fig. 3. Effect of modulating μ-opioid receptor (MOR) neurons in the periaqueductal gray (PAG) on escape behaviors. (*A*) Approach to chemogenetically activate and inhibit MOR neurons in the PAG (PAG^{MOR}) after the injection of excitatory and inhibitory Cre-dependent designer receptor exclusively activated by designer drugs (DREADDs), respectively, to the PAG. A representative image is shown. *Scale bar* = 50 μm. (*B*) Induction of Fos expression within the rostral ventromedial medulla (RVM) after chemogenetic manipulation of PAG^{MOR} neurons. Representative images of RVM sections are shown. *Scale bar* = 50 μm. Comparison of Fos expression in the RVM. Data are mean ± SD with *dots* representing individual mice (n = 7 or 8 mice per group, averaging 4 sections per mouse). *P* values indicate the results of one-way ANOVA with Dunnett's multiple corrections test. (*C* to *E*) Effect of chemogenetic activation and inhibition on the (*C*) open field, (*D*) hotplate test examining total jumps and latency to jump, and (*E*) licking behaviors after intraplantar capsaicin-induced injury. Data are mean ± SD with *dots* representing individual mice (control: 6 to 11, modified form of the human M^3 muscarinic receptor (hM3Dq): 7 to 13, and modified form of the human M4 muscarinic receptor (hM4Di): 7 to 11 mice per group). *P* values indicate the results of one-way ANOVA with Dunnett's multiple corrections test. (*F*) Effect of chemogenetic manipulations of PAG^{MOR} neurons on licking responses after intraplantar formalin. Time course of licking responses binned every 5 min during 1 h. Data are mean ± SD (n = control: 11, Gq: 13, and Gi: 11 mice per group). (*G*) Cumulative data during 1 h and during the second phase of formalin-induced injury (11 to 60 min). Data are mean ± SD with *dots* representing individual mice (n = 11 to 13 mice per group). *P* values indicate the results of one-way ANOVA with Dunnett's multiple corrections test.

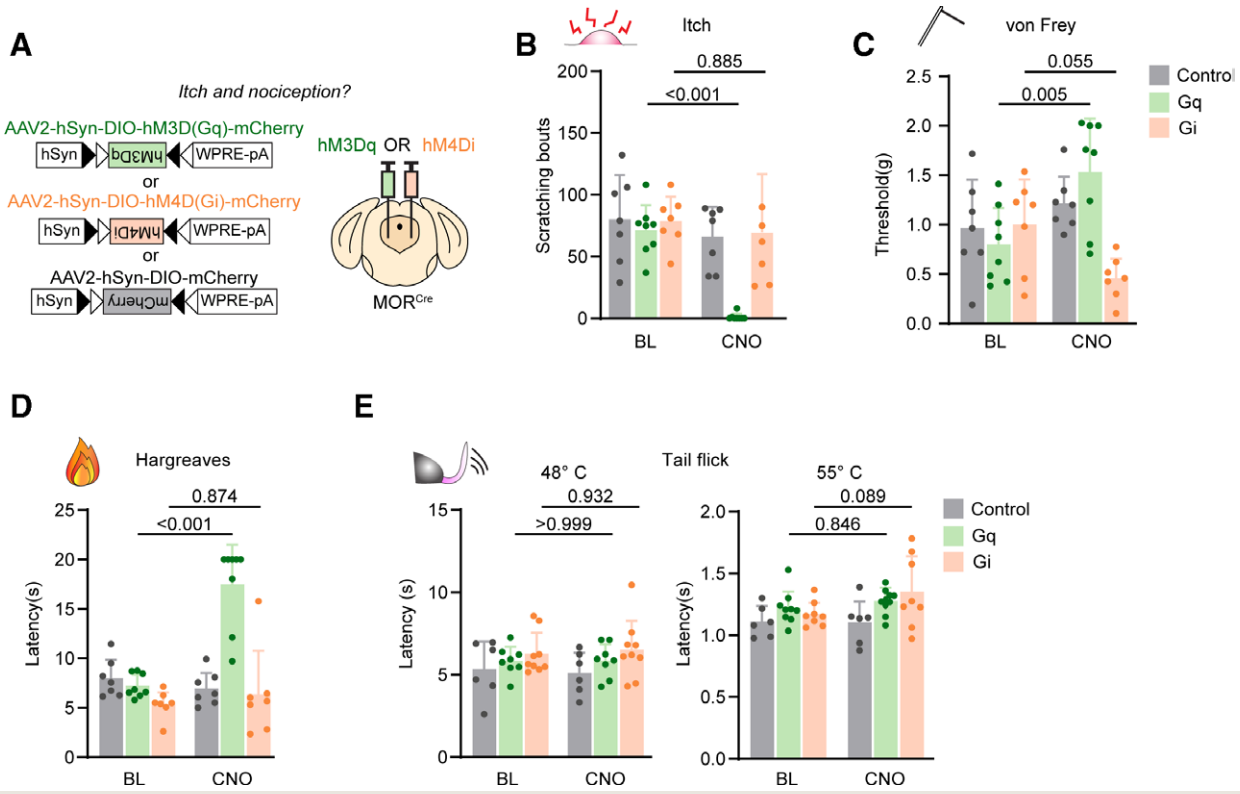

Fig. 4. μ-Opioid receptor (MOR) neurons in the (PAG) modulate itch and reflexive nociceptive behaviors. (*A*) Approach to chemogenetically activate and inhibit MOR neurons in the PAG (PAG^{MOR}) after the injection of excitatory and inhibitory Cre-dependent designer receptor exclusively activated by designer drugs (DREADDs), respectively, to the PAG. (*B* to *E*) Effect of chemogenetic manipulations of PAG^{MOR} neurons on (*B*) chloroquine-induced itch, (*C*) von Frey assay, (*D*) Hargreaves assay, and (*E*) tail flick assay at 48°C and 55°C. Data are mean ± SD with *dots* representing individual mice (control: 6 or 7, modified form of the human M^3 muscarinic receptor (hM3Dq): 8 or 9, and modified form of the human M4 muscarinic receptor (hM4Di): 7 or 8 mice per group). *P* values indicate the results of two-way repeated-measures ANOVA with Sidak's multiple corrections test.

excitation increased the latency to respond, consistent with reduced sensitivity. Last, the activation of PAG^{MOR} neurons robustly attenuated chloroquine-induced scratching. Thus, modulation of nociceptive behavior by activity in μ-opioid receptor–expressing neurons of the periaqueductal gray has differential effects on distinct nociceptive behaviors: threshold responses were reduced, and itch behavior was eliminated, but escape behavior was enhanced.

Modulation of Latent Sensitization by a Brainstem Circuit

The parabrachial nucleus has also been shown to engage descending modulatory systems for nociception.[29] We have previously examined the role of parabrachial nucleus projections to the periaqueductal gray in the facilitation of jumping behaviors.[24] Our previous observation supports the role of the parabrachial nucleus in the central modulation of nociception through a direct connection to the periaqueductal gray.[24] Building on this work, we tested a possible role for opioid-dependent signaling between the parabrachial nucleus and the periaqueductal gray.

We found that the systemic administration of naloxone (10 mg/kg intraperitoneal) in naive animals did not affect jumping behaviors (either latency to jump or total jumps) on the hotplate assay compared to that in saline-injected mice (latency: mean difference, −5.14 ± 4.58 s; 95% CI, −15.04 to 4.75; $P = 0.282$; and total jumps: mean difference, 4 ± 3 jumps; 95% CI, −2 to 11; $P = 0.183$ by unpaired *t* test; n = 10 mice per group; fig. 5A; Supplemental Figure 4A, https://links.lww.com/ALN/D202).

However, we were surprised to find that compared to baseline, the administration of naloxone facilitated jumping behaviors in mice that had undergone intracranial surgery 4 to 6 weeks before behavioral testing (fig. 5B). In these "control" mice (those having undergone surgery, but expressing eYFP alone rather than channelrhodopsin), naloxone decreased the latency to jump and increased total jumping behaviors (latency to jump: least-squares mean difference, 40.89 s; 95% CI, 30.15 to 51.62; $P < 0.001$; total jumps: least-squares mean difference, −12 jumps; 95% CI, −17 to −7; $P <$

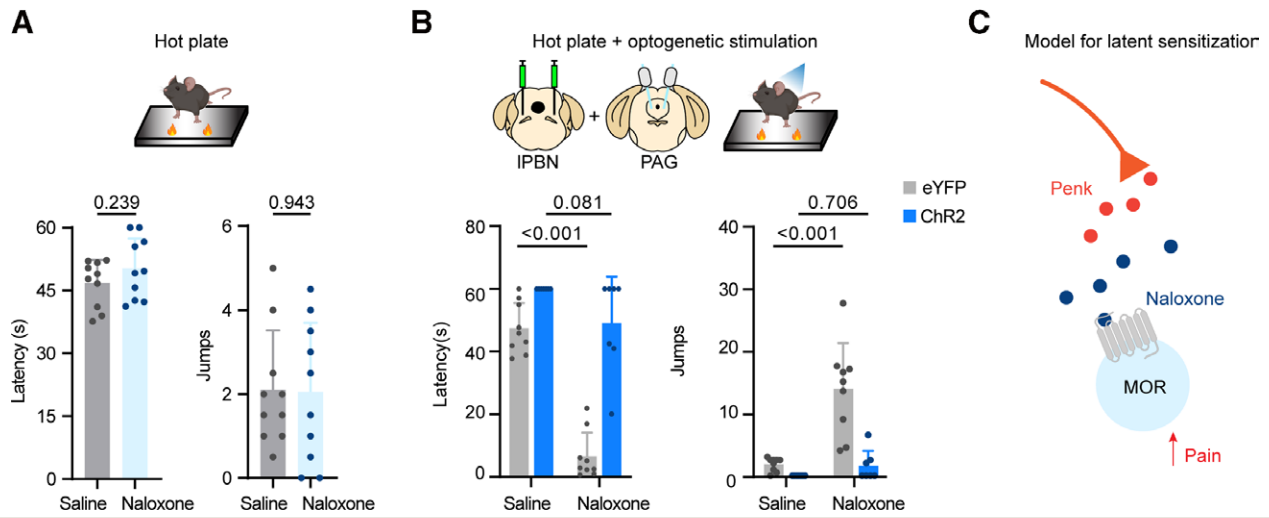

Fig. 5. Latent sensitization of pain is suppressed by stimulation of a parabrachial pathway within the periaqueductal gray (PAG). (*A*) Jumping behaviors among naive animals receiving saline or naloxone. Latency to jump and total jumps on a hotplate were quantified. Data are mean ± SD with *dots* representing individual mice (n = 10 mice per group). *P* values indicate the results of a two-tailed unpaired *t* test. (*B*) Effect of optogenetic stimulation of parabrachial nucleus (PBN) projections in the PAG in the presence of naloxone on hotplate jumping behaviors including (*C*) latency to jump and total jumps. Data are mean ± SD with *dots* representing individual mice (n = 7 to 9 mice per group). *P* values indicate the results of two-way repeated-measures ANOVA with Sidak's multiple comparisons test. (*C*) Model for compensatory endogenous opioid signaling after injury.

0.001 by two-way repeated-measures ANOVA with Sidak's multiple comparisons test; n = 9 mice; fig. 5C). Optogenetic photostimulation of parabrachial nucleus fibers within the periaqueductal gray reversed the effects of naloxone, namely the reduced jumping latency (least-squares mean difference, 10.92 s; 95% CI, −1.25 to 23.09; $P = 0.081$ by two-way repeated-measures ANOVA with Sidak's multiple comparisons test; n = 7 mice) and the naloxone-induced total jumps on the hotplate test (least-squares mean difference, −2 jumps; 95% CI, −7 to 4; $P = 0.706$ by two-way ANOVA with Sidak's multiple comparisons test; n = 7 mice). These findings suggest that photostimulation blocked the hyperalgesic effects of naloxone (fig. 5B; Supplemental Figure 4B, https://links.lww.com/ALN/D202).

The robust effects of naloxone in precipitating escape behaviors to hotplate testing in the absence of a previous injury (beyond the intracranial viral injection and implantation of optic fibers) highlight the role of compensatory endogenous opioid mechanisms that are engaged after cranial surgery. Endogenous opioid signaling has been shown to mask the behavioral expression of nociception in a variety of chronic and inflammatory models of pain in a process known as latent sensitization of pain.[30] After a noxious injury, animals exhibit a hypersensitive state that is later suppressed by compensatory upregulation of opioid signaling[31] (fig. 5C). This induction of the latent sensitization to noxious stimuli is unmasked after the application of opioid receptor antagonists, such as naloxone.[30] The striking attenuation of naloxone-induced hypersensitivity by optical stimulation of parabrachial nucleus terminals within the periaqueductal gray suggests its significant contribution to the modulation of opioid-dependent latent sensitization.

Discussion

Here, we used the *MOR*^{Cre} allele to examine the modulatory role of PAG^{MOR} neurons in models of nociceptive and itch behaviors. We found that activation of PAG^{MOR} neurons facilitated escape behaviors but inhibited reflexive responses to thermal and mechanical thresholds as well as responses to pruritogen-evoked itch. In addition, we tested the role of compensation by endogenous opioids within the periaqueductal gray for the maintenance of chronic postsurgical hypersensitivity. These data suggest that μ-opioid receptor–expressing neurons in the periaqueductal gray modulate nociception by eliciting distinct escape and reflexive responses.

It has recently been shown that the periaqueductal gray comprises several subpopulations of neurons that modulate nociception and itch.[18–20,32] In addition to differences in pharmacologic profiles,[1,33] Periaqueductal gray neurons have also been categorized by neurotransmitter class. GABAergic (*Vgat*), or inhibitory, neurons are thought to be pronociceptive, whereas glutamatergic (*Vglut2*), or excitatory, neurons are thought to be antinociceptive.[18,19,34] In our initial neurochemical characterization of PAG^{MOR} using fluorescent *in situ* hybridization, we found that *Oprm1* labeled a large number of both glutamatergic

and GABAergic neurons within the periaqueductal gray. These data precluded clear functional subclassifications of μ-opioid receptor–expressing neurons as these two neurochemically distinct populations have been shown to differentially mediate itch and nociception.[18,19,34] Therefore, we used a viral approach to label only PAG^{MOR} neurons that project to the rostral ventromedial medulla and performed a fluorescent *in situ* hybridization analysis of this subset of neurons. Although all the neurons back-labeled from the rostral ventromedial medulla were *Oprm1*$^{+}$, these neurons only represented about 25% of the total *Oprm1*-expressing population in the periaqueductal gray. Nevertheless, we consistently found that PAG^{MOR} neurons projecting to rostral ventromedial medulla expressed *Vglut2,* and optogenetic activation of this pathway was sufficient to induce Fos expression in the rostral ventromedial medulla. Our findings, therefore, argue that PAG^{MOR} neurons send primarily excitatory input to the rostral ventromedial medulla. In this study, we only characterized the neurotransmitter phenotype in the subset of rostral ventromedial medulla–projecting PAG^{MOR} neurons, which likely does not reflect all the output PAG^{MOR} neurons that could also modulate nociception. Additional neurotransmitter classifications of periaqueductal gray neurons projecting to structures other than the rostral ventromedial medulla remain to be fully characterized.

Dysregulation of functional connectivity between the periaqueductal gray and other supraspinal structures has been observed in preclinical and clinical models of chronic pain,[35] further underscoring the importance of the periaqueductal gray in different forms of acute as well as persistent pain. Plastic changes have been shown to occur within the periaqueductal gray in chronic pain, although we did not test the contributions of periaqueductal gray *MOR*^{Cre} neurons in a chronic model of pain. However, a surprising finding in our study was the role of a molecularly defined population in the periaqueductal gray expressing μ-opioid receptor in escape, reflexive, and itch behaviors. Based on pharmacologic studies of μ agonists and antagonists in the periaqueductal gray, we predicted that the optogenetic or chemogenetic activation of PAG^{MOR} neurons would have facilitated nociception, whereas chemogenetic inhibition of these neurons would have antinociceptive effects. We found that this paradigm was generally predictive when it came to strongly noxious or inflammatory stimuli and acute injury models. With hotplate testing, optogenetic and chemogenetic activation both elicited escape behaviors. We saw a similar trend with intraplantar capsaicin and formalin, although these trends did not reach statistical significance. We generally observed the opposite pattern with assays more commonly used to assess nociceptive thresholds. In contrast to the hotplate, formalin, and capsaicin assays, the von Frey and Hargreaves assays revealed that activation and inhibition of PAG^{MOR} neurons increased and decreased response thresholds, respectively.

One popular idea is that descending modulation inhibits (or facilitates) nociceptive input as it passes through the dorsal horn. In this context, our finding that seemingly opposing behavioral responses are observed upon manipulation of PAG^{MOR} neurons is confusing. Another possibility is that descending modulation alters the behavioral responses to noxious input. In this scenario, activity in the periaqueductal gray might selectively modulate diverse behavioral outputs in different ways, presumably through distinct neural targets. We found that PAG^{MOR} neurons inhibited reflexive thresholds upon von Frey and Hargreaves testing and facilitated escape behaviors with hotplate testing and licking in response to more noxious stimuli, such as capsaicin or formalin. We speculate that frankly noxious stimuli may induce an alarm state that exposes the role of PAG^{MOR} neurons in coordinating escape responses to noxious stimuli with the simultaneous suppression of reflexive responses. The conditions that engage periaqueductal gray neural circuits remain an important question. We have previously shown the importance of descending modulatory circuits involving the periaqueductal gray in modulating escape responses to pain[24] and stress-induced antinociception.[32] The periaqueductal gray is important for other physiologic systems of homeostatic regulation including autonomic control, aversion, and anxiety.[36,37] Stimulation of specific regions within the ventrolateral periaqueductal gray has been shown to elicit distinct behavioral responses[38] including locomotion as well as antinociception.[25] Therefore, we speculate that PAG^{MOR} neurons coordinate a defensive response to nociception; activation of these neurons suppresses sensitivity to threshold assays in favor of facilitating escape behaviors in noxious settings.

Activation of PAG^{MOR} neurons completely attenuated chloroquine-induced itch. This observation that periaqueductal gray neurons are dichotomously engaged for nociception and pruriception would align with recent work showing that both GABAergic and glutamatergic periaqueductal gray neurons divergently modulate behavioral responses to painful and itchy stimuli.[18,19] Our exploration into the function of periaqueductal gray circuitry using PAG^{MOR} neurons as an entry point supports the previous observation that neurons in the periaqueductal gray do not modulate all forms of nociception and pruriception in the same way. Our results reveal the contributions of PAG^{MOR} signaling in the modulation of itch behavior. Our findings that chemogenetic activation of PAG^{MOR} neurons suppresses itch suggest that these neurons may potentially be disinhibited by μ agonists, a mechanism that is consistent with one we previously described for neuraxial opioids, which elicit itch at the level of the spinal cord through a mechanism of disinhibition.[39] Our behavioral findings highlight opioid circuitry in the periaqueductal gray as a potential locus for the modulation of itch.

Chronic postsurgical pain is prevalent in 10 to 30% of postsurgical patients and is difficult to treat.[40] In rodent models, the suppression of mechanical and thermal hypersensitivity in

the weeks to months after injury has been shown to depend on the upregulation of opioid signaling.[30] Latent sensitization is thought to be maintained through opioid-dependent mechanisms at both spinal[30] and supraspinal[41,42] levels. In this study, we found that activation of parabrachial nucleus projections in the periaqueductal gray reversed naloxone-induced hypersensitivity in a postsurgical model of latent sensitization. We did not perform a classical injury model for latent sensitization (such as plantar incision, nerve injury, or complete Freund's adjuvant).[30,43] Instead, the administration of naloxone in animals that had previously received cranial implants of optical fibers and stereotactic viral injections was sufficient for the emergence of latent sensitization.

As previously proposed,[30] after injury, there is an upregulation of μ-opioid receptor signaling that is unmasked by the administration of naloxone. Although the precise mechanism by which this occurs was not explored in our study, we found that optical stimulation of the parabrachial nucleus output to the periaqueductal gray acutely suppresses the hypersensitivity induced by naloxone. We did not assess which surgical step(s) (such as drilling of the burr hole, lowering of the injector needle, or implantation of the optical fiber) could have contributed to the phenomenon of latent sensitization or the timeline during which latent sensitization develops after surgery. We also did not test the possibility that latent sensitization may involve an ascending or descending projection from the periaqueductal gray. Nevertheless, our current observations pose an important consideration for future studies using stereotactic delivery or intracranial implantation as these manipulations could also affect endogenous opioid signaling.

There has been considerable clinical interest in using the endogenous pain modulatory system for the management of pain disorders. Electrical stimulation of the periaqueductal gray has been reported to improve subjective ratings of pain in human studies.[44] Functional neuroimaging studies have consistently found that the periaqueductal gray is activated in models of placebo analgesia.[4–6] Our study focuses on the direct role of PAG^{MOR} neurons, which have been previously implicated as an important site for endogenous antinociception. Using preclinical models, we highlight the circuitry and behavioral role of the μ-opioid receptor–expressing subset of neurons in the descending modulatory pathway. We reveal the behavioral complexity of activating these neurons in the periaqueductal gray, which has important implications for how endogenous modulatory circuits are engaged for the behavioral expression of nociception. Finally, we acknowledge the important challenge of addressing whether the observed changes in pain (or itch) behaviors are truly paralleled by differences in the perceptual experience.

Acknowledgments

MOR^{Cre} mice were a generous gift from Richard Palmiter, Ph.D., (University of Washington, Seattle, Washington) and are now commercially available at Jax Labs (Harbor, Maine).

Research Support

Research reported in this publication was supported by National Institutes of Health and National Institute of Arthritis and Musculoskeletal and Skin Diseases (Bethesda, Maryland) grant AR063772, National Institutes of Health and National Institute of Neurological Disorders and Stroke (Bethesda, Maryland) grant NS096705 (to Dr. Ross), NRSA F31 grant F31NS113371, and National Institutes of Health and National Institute of General Medical Sciences (Bethesda, Maryland) grant T32GM008208 (to Dr. Nguyen).

Competing Interests

The authors declare no competing interests.

Correspondence

Correspondence to Dr. Ross: W1456 Biomedical Science Tower, 200 Lothrop St., Pittsburgh, Pennsylvania 15213. saross@pitt.edu.

Supplemental Digital Content

Supplemental Figure 1. Main figure 2 split by male and female sex, https://links.lww.com/ALN/D199
Supplemental Figure 2. Main figure 3 split by male and female sex, https://links.lww.com/ALN/D200
Supplemental Figure 3. Main figure 4 split by male and female sex, https://links.lww.com/ALN/D201
Supplemental Figure 4. Main figure 5 split by male and female sex, https://links.lww.com/ALN/D202

References

1. Moreau JL, Fields HL: Evidence for GABA involvement in midbrain control of medullary neurons that modulate nociceptive transmission. Brain Res 1986; 397:37–46
2. Behbehani MM, Fields HL: Evidence that an excitatory connection between the periaqueductal gray and nucleus raphe magnus mediates stimulation produced analgesia. Brain Res 1979; 170:85–93
3. Basbaum AI, Fields HL: Endogenous pain control mechanisms: Review and hypothesis. Ann Neurol 1978; 4:451–62
4. Eippert F, Bingel U, Schoell ED, Yacubian J, Klinger R, Lorenz J, Büchel C: Activation of the opioidergic descending pain control system underlies placebo analgesia. Neuron 2009; 63:533–43
5. Wager TD, Scott DJ, Zubieta J-K: Placebo effects on human mu-opioid activity during pain. Proc Natl Acad Sci USA 2007; 104:11056–61
6. Derbyshire SWG, Osborn J: Offset analgesia is mediated by activation in the region of the periaqueductal

grey and rostral ventromedial medulla. Neuroimage 2009; 47:1002–6
7. Lewis VA, Gebhart GF: Evaluation of the periaqueductal central gray (PAG) as a morphine-specific locus of action and examination of morphine-induced and stimulation-produced analgesia at coincident PAG loci. Brain Res 1977; 124:283–303
8. Carstens E, Hartung M, Stelzer B, Zimmermann M: Suppression of a hind limb flexion withdrawal reflex by microinjection of glutamate or morphine into the periaqueductal gray in the rat. Pain 1990; 43:105–12
9. Loyd DR, Wang X, Murphy AZ: Sex differences in micro-opioid receptor expression in the rat midbrain periaqueductal gray are essential for eliciting sex differences in morphine analgesia. J Neurosci 2008; 28:14007–17
10. Vigouret J, Teschemacher H, Albus K, Herz A: Differentiation between spinal and supraspinal sites of action of morphine when inhibiting the hindleg flexor reflex in rabbits. Neuropharmacology 1973; 12:111–21
11. Vaughan CW, Ingram SL, Connor MA, Christie MJ: How opioids inhibit GABA-mediated neurotransmission. Nature 1997; 390:611–4
12. Osborne PB, Vaughan CW, Wilson HI, Christie MJ: Opioid inhibition of rat periaqueductal grey neurones with identified projections to rostral ventromedial medulla in vitro. J Physiol (Lond) 1996; 490(pt 2):383–9
13. Budai D, Fields HL: Endogenous opioid peptides acting at mu-opioid receptors in the dorsal horn contribute to midbrain modulation of spinal nociceptive neurons. J Neurophysiol 1998; 79:677–87
14. Heinricher MM, Tavares I, Leith JL, Lumb BM: Descending control of nociception: Specificity, recruitment and plasticity. Brain Res Rev 2009; 60:214–25
15. Commons KG, Aicher SA, Kow LM, Pfaff DW: Presynaptic and postsynaptic relations of mu-opioid receptors to gamma-aminobutyric acid-immunoreactive and medullary-projecting periaqueductal gray neurons. J Comp Neurol 2000; 419:532–42
16. Reichling DB, Basbaum AI: Contribution of brainstem GABAergic circuitry to descending antinociceptive controls: I. GABA-immunoreactive projection neurons in the periaqueductal gray and nucleus raphe magnus. J Comp Neurol 1990; 302:370–7
17. Kalyuzhny AE, Wessendorf MW: Relationship of mu- and delta-opioid receptors to GABAergic neurons in the central nervous system, including antinociceptive brainstem circuits. J Comp Neurol 1998; 392:528–47
18. Samineni VK, Grajales-Reyes JG, Sundaram SS, Yoo JJ, Gereau RW: Cell type-specific modulation of sensory and affective components of itch in the periaqueductal gray. Nat Commun 2019; 10:4356
19. Samineni VK, Grajales-Reyes JG, Copits BA, O'Brien DE, Trigg SL, Gomez AM, Bruchas MR, Gereau RW: Divergent modulation of nociception by glutamatergic and gabaergic neuronal subpopulations in the periaqueductal gray. eNeuro 2017; 4:ENEURO.0129–16.2017
20. Gao Z-R, Chen W-Z, Liu M-Z, Chen X-J, Wan L, Zhang X-Y, Yuan L, Lin J-K, Wang M, Zhou L, Xu X-H, Sun Y-G: Tac1-expressing neurons in the periaqueductal gray facilitate the itch-scratching cycle via descending regulation. Neuron 2019; 101:45–59.e9
21. Taylor NE, Pei J, Zhang J, Vlasov KY, Davis T, Taylor E, Weng F-J, Van Dort CJ, Solt K, Brown EN: The role of glutamatergic and dopaminergic neurons in the periaqueductal gray/dorsal raphe: Separating analgesia and anxiety. eNeuro 2019; 6:ENEURO.0018–18.2019
22. Gan Z, Gangadharan V, Liu S, Körber C, Tan LL, Li H, Oswald MJ, Kang J, Martin-Cortecero J, Männich D, Groh A, Kuner T, Wieland S, Kuner R: Layer-specific pain relief pathways originating from primary motor cortex. Science 2022; 378:1336–43
23. Huang J, Gadotti VM, Chen L, Souza IA, Huang S, Wang D, Ramakrishnan C, Deisseroth K, Zhang Z, Zamponi GW: A neuronal circuit for activating descending modulation of neuropathic pain. Nat Neurosci 2019; 22:1659–68
24. Chiang MC, Nguyen EK, Canto-Bustos M, Papale AE, Oswald A-MM, Ross SE: Divergent neural pathways emanating from the lateral parabrachial nucleus mediate distinct components of the pain response. Neuron 2020; 106:927–939.e5
25. Yu W, Pati D, Pina MM, Schmidt KT, Boyt KM, Hunker AC, Zweifel LS, McElligott ZA, Kash TL: Periaqueductal gray/dorsal raphe dopamine neurons contribute to sex differences in pain-related behaviors. Neuron 2021; 109:1365–1380.e5
26. Prieto GJ, Cannon JT, Liebeskind JC: N. raphe magnus lesions disrupt stimulation-produced analgesia from ventral but not dorsal midbrain areas in the rat. Brain Res 1983; 261:53–7
27. Basbaum AI, Fields HL: The origin of descending pathways in the dorsolateral funiculus of the spinal cord of the cat and rat: further studies on the anatomy of pain modulation. J Comp Neurol 1979; 187:513–31
28. Gebhart GF: Opiate and opioid peptide effects on brain stem neurons: Relevance to nociception and antinociceptive mechanisms. Pain 1982; 12:93–140
29. Roeder Z, Chen Q, Davis S, Carlson JD, Tupone D, Heinricher MM: Parabrachial complex links pain transmission to descending pain modulation. Pain 2016; 157:2697–708
30. Corder G, Doolen S, Donahue RR, Winter MK, Jutras BL, He Y, Hu X, Wieskopf JS, Mogil JS, Storm DR, Wang ZJ, McCarson KE, Taylor BK: Constitutive μ-opioid receptor activity leads to long-term endogenous analgesia and dependence. Science 2013; 341:1394–9
31. Taylor BK, Corder G: Endogenous analgesia, dependence, and latent pain sensitization. Curr Topics Behav Neurosci 2014; 20:283–325

32. Nguyen E, Smith KM, Cramer N, Holland RA, Bleimeister IH, Flores-Felix K, Silberberg H, Keller A, Le Pichon CE, Ross SE: Medullary kappa-opioid receptor neurons inhibit pain and itch through a descending circuit. Brain 2022; 145:2586–601
33. Carstens E, Stelzer B, Zimmermann M: Microinjections of glutamate or morphine at coincident midbrain sites have different effects on nociceptive dorsal horn neurons in the rat. Neurosci Lett 1988; 95:185–91
34. Aimone LD, Gebhart GF: Stimulation-produced spinal inhibition from the midbrain in the rat is mediated by an excitatory amino acid neurotransmitter in the medial medulla. J Neurosci 1986; 6:1803–13
35. Mainero C, Boshyan J, Hadjikhani N: Altered functional magnetic resonance imaging resting-state connectivity in periaqueductal gray networks in migraine. Ann Neurol 2011; 70:838–45
36. Makovac E, Venezia A, Hohenschurz-Schmidt D, Dipasquale O, Jackson JB, Medina S, O'Daly O, Williams SCR, McMahon SB, Howard MA: The association between pain-induced autonomic reactivity and descending pain control is mediated by the periaqueductal grey. J Physiol (Lond) 2021; 599:5243–60
37. Fernandes GG, Frias AT, Spiacci A, Pinheiro LC, Tanus-Santos JE, Zangrossi H: Nitric oxide in the dorsal periaqueductal gray mediates the panic-like escape response evoked by exposure to hypoxia. Prog Neuropsychopharmacol Biol Psychiatry 2019; 92:321–7
38. Behbehani MM: Functional characteristics of the midbrain periaqueductal gray. Prog Neurobiol 1995; 46:575–605
39. Nguyen E, Lim G, Ross SE: Evaluation of therapies for peripheral and neuraxial opioid-induced pruritus based on molecular and cellular discoveries. Anesthesiology 2021; 135:350–65
40. Bruce J, Quinlan J: Chronic post surgical pain. Rev Pain 2011; 5:23–9
41. Cooper AH, Hedden NS, Corder G, Lamerand SR, Donahue RR, Morales-Medina JC, Selan L, Prasoon P, Taylor BK: Endogenous μ-opioid receptor activity in the lateral and capsular subdivisions of the right central nucleus of the amygdala prevents chronic postoperative pain. J Neurosci Res 2022; 100:48–65
42. Porreca F, Ossipov MH, Gebhart GF: Chronic pain and medullary descending facilitation. Trends Neurosci 2002; 25:319–25
43. Marvizon JC, Walwyn W, Minasyan A, Chen W, Taylor BK: Latent sensitization: A model for stress-sensitive chronic pain. Curr Protoc Neurosci 2015; 71:9.50.1–9.50.14
44. Fardin V, Oliveras JL, Besson JM: A reinvestigation of the analgesic effects induced by stimulation of the periaqueductal gray matter in the rat. II. Differential characteristics of the analgesia induced by ventral and dorsal PAG stimulation. Brain Res 1984; 306:125–39